Korean J Physiol Pharmacol
Vol 9: 131-135, April, 2005

Modulation of Large Conductance Ca^{2+}-activated K^+ Channel of Skin Fibroblast (CRL-1474) by Cyclic Nucleotides

Jihyun Yun, Seungtae Kim, and Hyoweon Bang

Department of Physiology, College of Medicine, Chung-Ang University, Seoul 156-756, Korea

Potassium channels in human skin fibroblast have been studied as a possible site of Alzheimer disease pathogenesis. Fibroblasts in Alzheimer disease show alterations in signal transduction pathway such as changes in Ca^{2+} homeostasis and/or Ca^{2+}-activated kinases, phosphatidylinositol cascade, protein kinase C activity, cAMP levels and absence of specific K^+ channel. However, little is known so far about electrophysiological and pharmacological characteristics of large-conductance Ca^{2+}-activated K^+ (BK_{Ca}) channel in human fibroblast (CRL-1474). In the present study, we found Iberiotoxin- and TEA-sensitive outward rectifying oscillatory current with whole-cell recordings. Single channel analysis showed large conductance K^+ channels (106 pS of chord conductance at +40 mV in physiological K^+ gradient). The 106 pS channels were activated by membrane potential and $[Ca^{2+}]_i$, consistent with the known properties of BK_{Ca} channels. BK_{Ca} channels in CRL-1474 were positively regulated by adenylate cyclase activator (10 μM forskolin), 8-Br-cyclic AMP (300 μM) or 8-Br-cyclic GMP (300 μM). These results suggest that human skin fibroblasts (CR-1474) have typical BK_{Ca} channel and this channel could be modulated by c-AMP and c-GMP. The electrophysiological characteristics of fibroblasts might be used as the diagnostic clues for Alzheimer disease.

Key Words: BK_{Ca} channel, Fibroblast, Alzheimer disease, Second messenger system, cAMP, cGMP

INTRODUCTION

K^+ channels allow K^+ ions to selectively pass through the cell membrane. These channels counteract the activities of Na^+ and Ca^{2+} channels in controlling cell excitability and are grouped into several families, including voltage-gated K^+ channels, inwardly rectifying K^+ channels and two-pore K^+ channels (Wallner et al, 1999).

The family of voltage-gated K^+ channels includes Ca^{2+}-activated K^+ channels of large (BK), intermediate (IK), and small conductance (SK). The single channel conductance of BK_{Ca} channels is ~250 pS in 140 mM symmetrical K^+, whereas it is only ~110 pS under physiological conditions (5 mM K^+ outside, 140 mM K^+ inside). It is generally known as maxi-K^+ channel, because of its huge conductance. BK_{Ca} channel is enriched in synaptic terminals and axons (Knaus et al, 1996), where it facilitates membrane repolarization during an action potential, thereby participating in the regulation of neurotransmitter release (Gho & Ganetzky, 1992; Bielefeldt & Jackson, 1994). In addition, genetic and molecular approaches have demonstrated that BK_{Ca} channel is key determinant of certain behaviors-an inducible sticky-feet phenotype, a constitutive flight defect, and an altered mating song- in *Drosophila* (Atkinson et al, 2000; Brenner et al, 2000). BK_{Ca} channel is mainly activated by voltage and free intracellular calcium, and the channel activity may be also modulated by phosphorylation, depending on the particular protein kinase involved and the specific sites or combination of sites that are phosphorylated (Garcia & Kaczorowski, 1992; Breitwieser, 1996, Klrke et al, 1996).

In Alzheimer disease (AD), fibroblasts show altered in signal transduction pathways such as changes in Ca^{2+} homeostasis and/or Ca^{2+}-activated kinases, phosphatidylinositol cascade, protein kinase C activity, cAMP levels (Malow et al, 1989; Martinez et al, 1999), β-adrenergic-coupled formation of cAMP (Huang & Gibson, 1993) and K^+ channel activities (Etcheberrigaray et al, 1993). All or each of them are implicated as causative factor in AD. Since the fibroblasts can easily be obtained from human subject, an alteration of ion channel activity in skin fibroblasts can be a useful diagnostic tool for AD patient.

This study was undertaken to investigate the existence of BK_{Ca} channel in human skin fibroblast cell line CRL-1474 and to elucidate the electrophysiological properties and modulation mechanisms of BK_{Ca} channel.

METHODS

Cell culture

CRL-1474 cells, human skin fibroblast cell line, were

Corresponding to: Hyoweon Bang, Department of Physiology, College of Medicine, Chung-Ang University, 221 Heukseok-dong, Dongjak-gu, Seoul 156-756, Korea. (Tel) 82-2-820-5650, (Fax) 82-2-817-7115, (E-mail) haena@cau.ac.kr

ABBREVIATIONS: cAMP, cyclic adenosine monophosphate; cGMP, cyclic guanosine monophosphate; IbTX, Iberiotoxin; TEA, tetraethylammonium; PKA, protein kinase A; PKG, protein kinase G.

seeded in 35 mm culture dishes in Dulbecco's modified Eagle's medium (DMEM; JBI), supplemented with 10% fetal bovine serum (FBS: GIBCO), and passage 6 or 7 cells were used for this experiment.

If cells were sufficiently recovered, they were separated with trypsin/EDTA treatment. Separated cells were transferred to 13 mm glass cover slips and incubated for more than 2 hours at room temperature. The coverslips were coated with poly-L-lysine for best attachment of fibroblast cells.

Electrophysiological recordings

For patch-clamp experiments, the cultured CRL-1474 cells on the coverslips were transferred to a recording chamber on the stage of an inverted microscope. The external solution was applied by a microperfusion system (0.5 ml/min) that consisted of ten teflon tubes arranged in parallel in one plane and aligning various barrels for changing solutions. All experiments were performed at room temperature. Recording pipettes were made of borosilicate glass (WPI, MTW 150F-4) with electrode puller (Narishige, PP-83) and had resistances of 2 ~ 4 MΩ after fire polishing with Microforge (Narishige, MF-83).

Currents were recorded by using Axopatch 200B (Axon Instruments, USA). In the whole cell mode, series resistance was compensated at least 70~80% without significant oscillations in the current trace. All experiments began by recording of control currents without addition of any drug to the cells. Only cells with stable currents were used for analyses. K^+ currents were recorded by applying 400 ms steps to various command potentials (−60~+50 mV, holding potential was −70 mV). Single channel recordings were performed using inside-out and cell-attached patch-clamp technique. Analyses of single channel data were performed by measuring the unitary current amplitudes and channel activity (*NPo*), where *N* is the number of functional channels and *Po*, the open-state probability. In the majority of single-channel recordings, one to two channels were observed under control conditions. Whole-cell and single channel currents were filtered at 2 kHz and digitized at 10 KHz. Data were analyzed and figured by using Clampfit 9.0 (Axon Instruments, USA) and origin 7.0 (Origin Lab Corporation, USA) software.

Solutions and drugs

Whole-cell experiments were performed in normal Tyrode solution with the following composition (mM): 145 NaCl, 5 KCl, 1 $CaCl_2$, 1 $MgCl_2$, and 10 HEPES (pH 7.3 with NaOH). The patch pipette contained (mM): 145 KCl, 1.013 $MgCl_2$, 2 EGTA, 2 K-ATP, and 10 HEPES (pCa 6.0, pH 7.3 with KOH).

In the cell-attached path mode, the bath and the pipette solutions were normal Tyrode solution. For excised inside-out patch mode, the patches were bathed in the high K^+ solution; 145 KCl, 1 $MgCl_2$, 2 EGTA, and 10 HEPES (pH 7.3 with KOH). The free concentrations of Ca^{2+} in the solution containing chelating agents (EGTA) were estimated using the chelating program (designed by Theo JM Schoenmakers). The patch pipette solution was same as whole-cell perfusion solution. All drugs were applied by bath perfusion. Iberiotoxin (IbTx), tetraethylammonium (TEA), 8-Br-cAMP and 8-Br-cGMP were obtained from Sigma (St. Louis, USA). Forskolin was obtained from Biomol (Hamburg, Germany) and was used at 10 μM concentration.

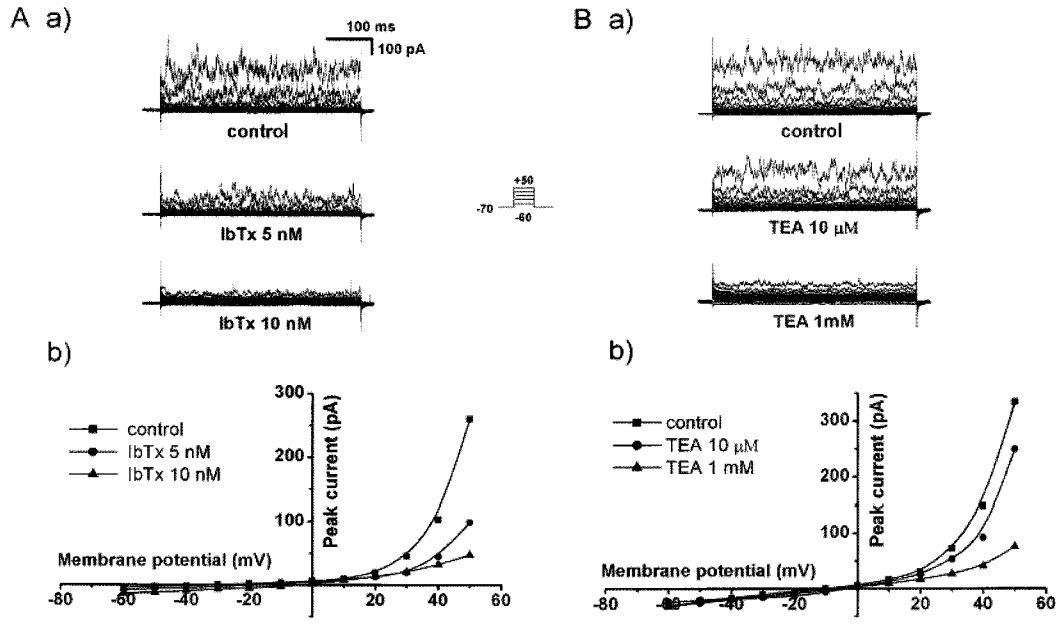

Fig. 1. Representative currents in human skin fibroblast cell line (CRL-1474) after stimulation with different voltage pulses (−60 to 50 mV) by whole-cell mode patch clamp techniques (holding potential was −70 mV) (Aa and Ba). The outward currents were activated around −10 mV and showed typical outward rectification. A significant fraction of the outward current was blocked by Iberiotoxin (IbTX) and tetramethylammonium (TEA), dose dependently (Ab and Bb).

RESULTS

Whole-cell recordings of BK_{Ca} channel in whole cell configuration

Fig. 1 shows typical examples of the outwardly rectifying whole-cell K^+ currents recorded from Human skin fibroblast cell line CRL-1474. The cell was bathed in 5 mM K^+, and the recording pipette solution contained 145 mM K^+ and pCa 6 (free Ca^{2+} concentration was 1 μM). The outward currents were activated at around −10 mV and showed typical outward rectification throughout the test pulses above −10 mV. The outward currents became very noisy and oscillated with strong depolarization (> +10 mV) (Fig. 1).

Iberiotoxin (IbTx) is a specific blocker of BK_{Ca} channels (K_d of IbTx ~ 1 nM, Wallner et al, 1999). A significant fraction of the outward currents, especially oscillatory components, were blocked dose-dependently by IbTx added to the bath solution. The outward current was decreased by 63±15. 4% with 5 nM IbTx and 83±8.7% with 10 nM IbTx (n=3) at +50 mV command potential (Fig. 1A).

The whole cell outward currents were also blocked by TEA dose-dependently. The oscillatory outward current was blocked by 34±7.3% with 10 μM TEA and 81±9.2% with 1 mM TEA (n=3) added to the bath at +50 mV command potential (Fig. 1B).

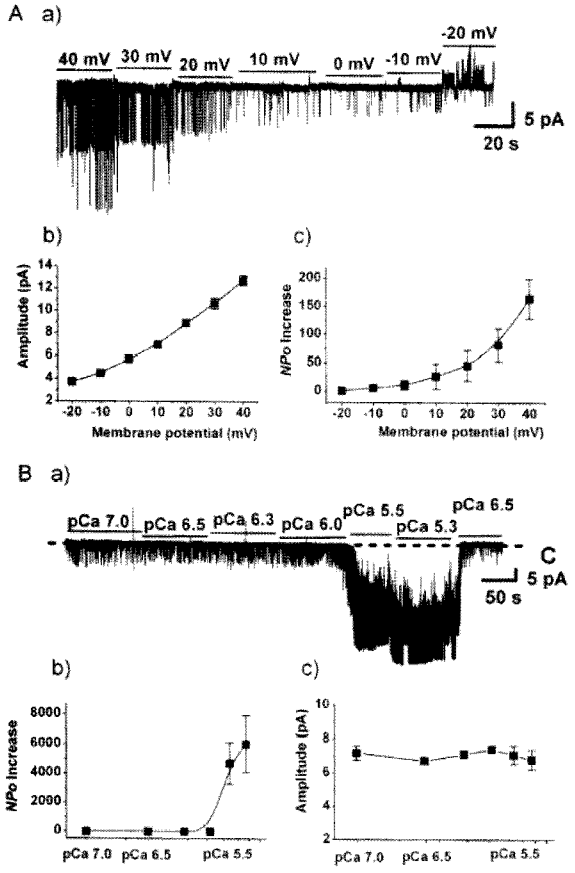

Fig. 2. Effects of membrane voltage and $[Ca^{2+}]_i$ on single-channel activities in the inside-out recording. (A) a. The single channel opened at the different holding potentials. Rapidly flickering single-channel currents with burst of activities separated by silent interburst periods. b. The single-channel current-voltage relationship was almost linear in the voltage range from +10 mV to +40 mV. c. Depolarization resulted in an increased channel activity. (B) a. Stepwise increases of $[Ca^{2+}]_i$ resulted in increases in channel activities. b. The relation between channel activities (*NPo*) and $[Ca^{2+}]_i$. *NPo* was increased by 4700 times at pCa 5.3 compare to pCa 7.0. EC_{50} value of 2.25 μM was calculated for the half-maximal channel activation. c. Unitary current amplitudes of the channel were not dependent on $[Ca^{2+}]_i$.

Single channel recordings of BK_{Ca} channel in the inside-out configuration

The recordings in each patch were made at different holding voltages, ranging from −20 mV to +40 mV. The current-voltage relationship of single channel currents in excised inside-out patches was measured in the recording pipette solution containing 5 mM KCl and 1 mM Ca^{2+}, and the bath solution containing 145 mM KCl and 1 μM free $CaCl_2$ (fixed with 2 mM EGTA) (Fig. 2A).

Fig. 2Aa shows rapidly flickering single channel currents with burst of activities separated by silent interburst periods. Under asymmetrical K^+ condition and absence of Na^+ on the cytoplasmic side of the patch, the single channel current-voltage relationship was almost linear in the voltage range from +10 mV to +40 mV or slightly outwardly rectified through the whole range of voltage. The single channel current-voltage (I~V) relation is plotted in Fig. 2Ab. Unitary current amplitudes of the channel were dependent on patch potential. Mean values of four independent experiments were 4.5±0.09 and 12.8±0.44 pA at −10 and +40 mV, corresponding to chord conductance of 64 and 106 pS, respectively. Channel activity measured by the number of open probability (*NPo*) was strongly voltage dependent. Depolarization resulted in an increased channel activity. In asymmetrical K^+ solutions at 1 μM $[Ca^{2+}]_i$, the *NPo* was 0.092±0.0745, 0.366±0.1785 and 1.48±0.295 at 0, +20 and +40 mV, respectively (n=4) (Fig. 2Ac).

Channel activity measured in inside-out patches showed strong dependence on the cytoplasmic side of $[Ca^{2+}]$ (Fig. 2B). At $[Ca^{2+}]_i$ of 0.3 μM (pCa 6.5), the patches displayed little channel activities. Stepwise increases of $[Ca^{2+}]_i$ from 0.5 μM (pCa 6.3) to 5 μM (pCa 5.3) resulted in an increase of channel activities from basal *NPo* of 0.0011±0.00053 to a maximal *NPo* of 4.97±0.408 (n=3) (about 4,700 times increase). Fig. 2Bb) shows the relationship between channel activity (*NPo*) and $[Ca^{2+}]_i$. The data were fitted with Hill's equation. At a membrane potential of +20 mV, EC_{50} value of 2.25 μM was calculated for thehalf-maximal channel activation. Unitary current amplitudes of the channel were not dependent on $[Ca^{2+}]_i$ (Fig. 2Bc).

Effect of cyclic nucleotides on the BK_{Ca} channel

We investigated effects of cyclic nucleotides on BK_{Ca} channel property in CRL-1474 with attached patch recordings. In particular, we sought to determine whether BK_{Ca} channel could be modulated by cAMP and cGMP. Stimulation of cells with forskolin, cAMP activator (an activator of adedylate cyclase), caused a marked increase in the activity of BK_{Ca} channel. Forskolin (10 μM) increased open probability (*NPo*) from 0.004±0.0012 to 0.081±0.037 (n=3). However single-channel conductance was not changed (Fig. 3). To confirm whether these currents were activated by

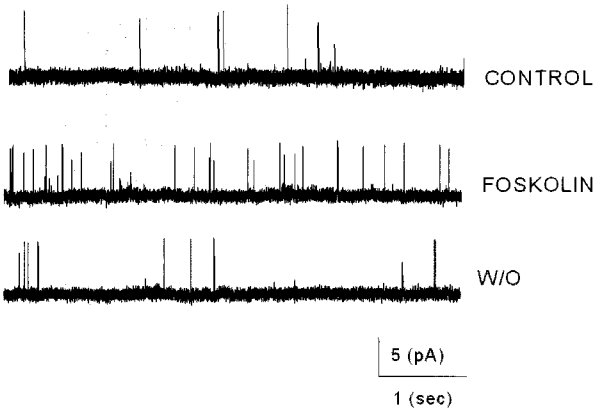

Fig. 3. The effect of forskolin on single channel activities in attached mode. Channel activity was continuously recorded from the same patch before (as control) and 5 to 8 min after application of drugs. Exposure of fibroblast to forskolin at a concentration of 10 μM increased the channel activities at a patch potential was +60 mV. Normal Ringer solution was used for the bath and pipette solution.

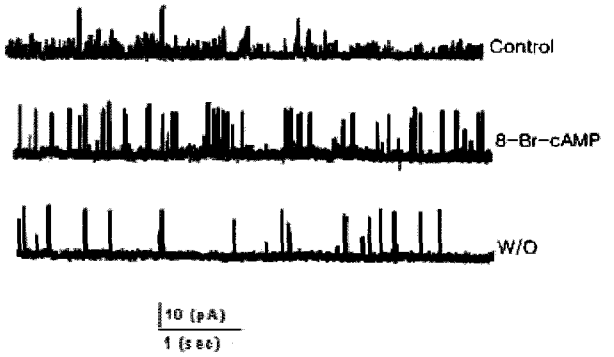

Fig. 4. The effects of 8-Br-cAMP on single channel activities in attached mode of patch clamp recording. 8-Br-cAMP (300 μM) increased the channel activities at a patch potential of +60 mV. The bath solution and pipette solution were normal Tyrode solution.

cAMP, we also tested membrane permeable analogue of cAMP.

As shown in Fig. 4, application of 8-Br-cyclic AMP (300 μM) to the bath solution of the attached patch increased *NPo* from 0.005±0.0015 to 0.13±0.032 (n=4). The single channel conductance and open time duration did not change and *NPo* was increased by the increase of open frequency.

Under the same condition, the application of 8-Br-cyclic GMP (300 μ) to the bath solution of the attached patch increased *NPo* in four out of five tested cells (Fig. 5). In those four cells, the *NPo* was increased from 0.003±0.0017 to 0.082±0.0335 (n=4) by increase of open frequency, however, single channel conductance and open time duration did not change.

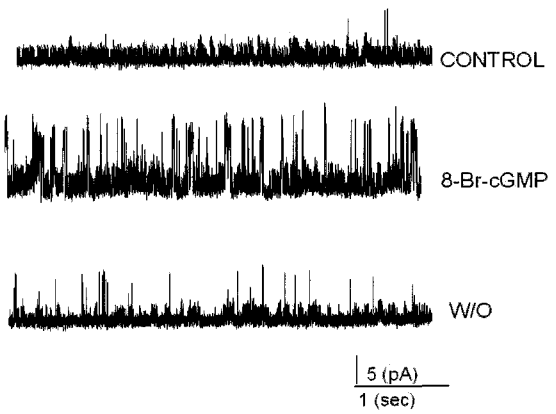

Fig. 5. The effects of 8-Br-cGMP on the single channel activities in attached mode of patch clamp recording. 8-Br-cGMP (300 μM) increased the channel activities at a patch potential of +60 mV. The bath solution and pipette solution were normal Tyrode solution.

DISCUSSION

In this study, we found BK_{Ca} channel in human skin fibroblast cell line (CRL-1474). In the whole-cell recordings, the iberiotoxin-sensitive outwardly rectifying currents were regarded as the BK_{Ca} currents. The outward currents were activated at around −20 mV and well maintained throughout the test pulses. The outward currents became very noisy and oscillated with strong depolarization. The mean current-voltage relationship (I~V) showed weak outward rectification.

A significant fraction of the outward currents especially oscillatory components, were blocked dose-dependently by IbTX added to the bath solution. The outward currents found in this study were more resistant to IbTX because only 63% of the current was decreased with 5 nM IbTX. TEA is an another potent blocker of BK_{Ca}. The whole cell outward currents were also blocked dose-dependently by TEA. The oscillatory outward current was blocked by 34% with 10 μM TEA in the bath at +50 mV command potential.

BK_{Ca} channel has large conductance (100~250 pS) and activation of the channel varies over a wide range of Ca^{2+} concentration from 100 nM to 10 μM (Latorre et al, 1989). Our results in the inside-out patches of fibroblasts showed large unitary currents with a chord conductance of around 105 pS at +40 mV in 1.0 μM Ca^{2+} in the bath solution. The open probability of BK_{Ca} in this study was increased by membrane depolarization as well as by increasing $[Ca^{2+}]_i$. Ca^{2+} sensitivity of BK_{Ca} channels varies markedly, depending on different tissues (Latorre et al, 1989). In the present study, a $[Ca^{2+}]_i$ of half maximal activation of this channel at +20 mV was calculated to be 2.25 μM. It is different from the values obtained in other cell types such as porcine endothelial cells (Baron et al, 1996), human endothelial cells (Khler et al, 1998), and bovine mesenteric vascular smooth muscle cells (Sansom & Stockand, 1994) which have half- maximal activation at 4.5 μM, 5.9 μM, and 0.2 μM, respectively. Therefore, the sensitivity to $[Ca^{2+}]_i$ of BK_{Ca} channel in fibroblast appears to be more sensitive than those in endothelial cell and less sensitive than those in vascular smooth muscle cells. The channel activities were significantly decreased after exposing cells to low concen-

trations of TEA or IbTX in the outside-out mode of patches (data not shown), which was consistent with the results of whole-cell recordings. Therefore, we can conclude that the outwardly rectifying K^+ currents recorded in the fibroblast (CRL-1474) are similar to those recorded in endothelial cells (Baron et al, 1996; Köhler et al, 1998) and vascular smooth muscle cells (Sansom & Stockand, 1994; Nelson & Quayle, 1995).

In smooth muscle cells, cyclic AMP activated by adenylate cyclase activators (isoprenaline and forskolin, etc.) increases BK_{Ca} channel activities, causing vascular relaxation. In the cell-attached recordings, BK_{Ca} channel activities in CRL-1474 were also increased by forskolin (Fig. 3), or by the addition of 300 μM 8-Br-cAMP to the bath solution (Fig. 4). Therefore we suggest that cAMP is also a participant in the signal transduction of BK_{Ca} regulation in fibroblasts.

It is generally assumed that cAMP acts only through the activation of protein kinase A (PKA) and cGMP only through the activation of protein kinase G (PKG), however, a growing number of studies suggest a process of crosstalk between the cAMP and cGMP signaling pathways: cAMP cross-activates PKG and stimulates BK_{Ca} channels in coronary artery smooth muscle (White et al, 2000), pulmonary arterial smooth muscle and bovine pulmonary arteries (Dhanakoti et al, 2000) and other vascular smooth muscle cells (Lincoln et al, 1990). In CRL-1474 cells, the *NPo* of BK_{Ca} channel was also increased by the addition of 300 μM 8-Br-cGMP (Fig. 5). In one of five experiments, however, 8-Br-cGMP did not change the *NPo* of BK_{Ca} channel (data not shown). Therefore, cGMP seems to have variable signal transduction mechanism than cAMP, and whether the changes of BK_{Ca} channel activity are mediated by crosstalk between cAMP and cGMP signaling pathway remains unclear.

In AD patients, it has been reported that K^+ channel activities change according to progression of the disease and these activities sometimes change before the onset of overt clinical symptoms. These include switching off of a K^+ channel, which is active at the resting membrane potential (Etcheberrigaray et al, 1993). However, very little is known about basic ion channel physiology involved.

In conclusion, our results demonstrate that human skin fibroblasts contain BK_{Ca} channels that are positively regulated by cAMP and cGMP. The examination of BK_{Ca} activity in the fibroblasts might provide a useful diagnostic tool for various human diseases, including AD.

ACKNOWLEDGEMENT

This research was supported by the Chung-Ang University Research Grants in 2001.

REFERENCES

Atkinson N, Brenner R, Chang W-M, Wilbur JL, Larimer JL, Yu J. Molecular separation of two behavioral phenotypes by a mutation affecting the promoters of a Ca^{2+}-activated K^+ channel. *J Neurosci* 20: 2988–2993, 2000

Baron A, Frieden M, Chabaud F, Beny JL. Ca^{2+}-dependent nonselective cation and potassium channels activated by bradykinin in pig coronary artery endothelial cells. *J Physiol (Lond)* 493: 691–706, 1996

Bielefeldt K, Jackson MB. Phosphorylation and dephosphorylation modulate a Ca^{2+}-activated K^+ channel in rat peptidergic nerve terminals. *J Physiol (Lond)* 475: 241–254, 1994

Breitwieser GE. Mechanisms of K^+ channel Regulation. *J Memb Biol* 152: 1–11, 1996

Brenner R, Yu JY, Srinivasan K, Brewer L, Larimer JL, Wilbur JL, Atkinson NS. Complementation of physiological and behavioral defects by a slowpoke Ca^{2+}-activated K^+ channel transgene. *J Neurochem* 75: 1310–1319, 2000

Dhanakoti SN, Gao Y, Nguyen MQ, Raj JU. Involvement of pulmonary arteries to cGMP and cAMP. *J Appl Physiol* 88: 1637–1642, 2000

Etcheberrigaray R, Ito E, Oka K, Tofel-Grehl B, Gibson G, Alkon DL. Potassium channel dysfunction in fibroblasts identifies patients with Alzheimer disease. *Proc Natl Acad Sci USA* 90: 8209–8213, 1993

Garcia ML, Kaczorowski GJ. High conductance calcium-activated potassium channels: molecular pharmacology, purification and regulation In: Weston AH, Hamilton TC ed, *Potassium Channel Modulators*. Blackwell Scientific Publications, Oxford, p 76–109, 1992

Gho M, Ganetzky B. Analysis of repolarization of presynaptic motor terminals in Drosophilia larvae using potassium channel-blocking drugs and mutations. *J Exp Biol* 170: 93–111, 1992

Horsburgh K, Daitoh T. Altered signal transduction in Alzheimer's disease, In: Terry RD, Katzman R, Bick KL ed, *Alzheimer's Disease*. Raven Press, New York, p 387–404, 1994

Huang HM, Gibson GE. Altered β-adrenergic receptor-stimulated cAMP formation in cultured skin fibroblasts from Alzheimer donors. *J Biol Chem* 268: 14616–14621, 1993

Klæke DA, Wienert H, Zeuthen T, J φgensen PL. Regulation of Ca^{2+}-activated K^+ channel from rabbit distal colon epithelium by phosphorylation and dephosphorylation. *J Membrane Biol* 151: 11–18, 1996

Knaus HG, Schwarzer C, Koch RO, Eberhart A, Kaczorowske GJ, Glossmann H, Wunder F, Pongs O, Garcia ML, Sperk G. Distribution of high-conductance Ca^{2+}-activated K^+ channels in rat brain:targeting to axons and nerve terminals. *J Neurosci* 16: 955–963, 1996

Köhler R, Schöngelder G, Hopp H, Distler A, Hoyer J. Stretch-activated cation channel in human umbilical vein endothelium in normal pregnancy and in preeclampsia. *J Hypertens* 16: 1149–1156, 1998

Latorre R, Oberhauser A, Labarca P, Alvarez O. Varieties of calcium-activated potassium channels. *Annu Rev Physiol* 51: 385–399, 1989

Lincoln TM, Cornwell TL, Taylor AE. cGMP-dependent protein kinase mediates the reduction of Ca^{2+} by cAMP in vascular smooth muscle cells. *Am J Physiol* 258: C399–407, 1990

Malow BA, Baker AC, Blass JP. Cultured cells as a screen for novel treatments of Alzheimer's disease. *Arch Neurol* 46: 1201–1203, 1989

Martinez M, Fernandez E, Frank A, Guaza C, De la Fuente M, Hernanz A. Increased cerebrospinal fluid cAMP levels in Alzheimer's disease. *Brain Res* 846: 265–267, 1999

Nelson MT, Quayle JM. Physiological roles and properties of potassium channels in arterial smooth muscle. *Am J Physiol* 268: C799–822, 1995

Sansom SC, Stockand JD. Differential Ca^{2+} sensitivities of BK_{Ca} isochannels in bovine mesenteric artery. *Am J Physiol* 266: C1182–1189, 1994

Wallner M, Meea P, Toro L. Calcium-activated potassium channels in muscle and brain. In: Kurachi Y, Jan LY, Lazdunski M ed, *Potassium Ion Channels; Molecular Structure, Function and Diseases*. Acdemic Press, San Diego, p 117–140, 1999

White RE, Kryman JP, El-Mowafy A, Han G, Carrier GO. cAMP-dependent vasodilators cross-activate the cGMP dependent protein kinase to stimulate BK_{Ca} channel activity in coronary artery smooth muscle. *Circ Res* 86: 897–905, 2000

Erratum

Kor J Physiol Pharmacol 9: 55-62, 2005.

Effect of Extracts from Safflower Seeds on Osteoblastic Differentiation and Intracellular Free Calcium Concentration in MC3T3-E1 Cells

Hye-Ock Jang, et al

Figure 6~10 were misprinted. The figures should appear as follows:

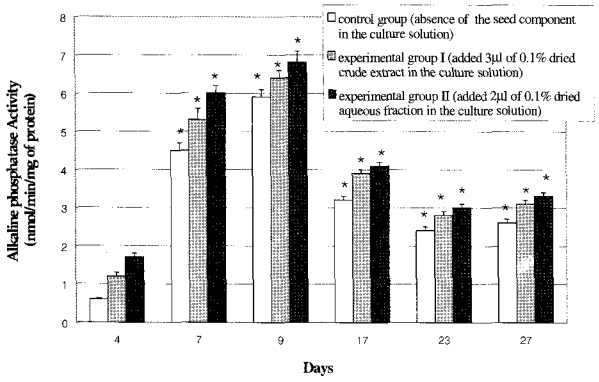

Fig. 6.

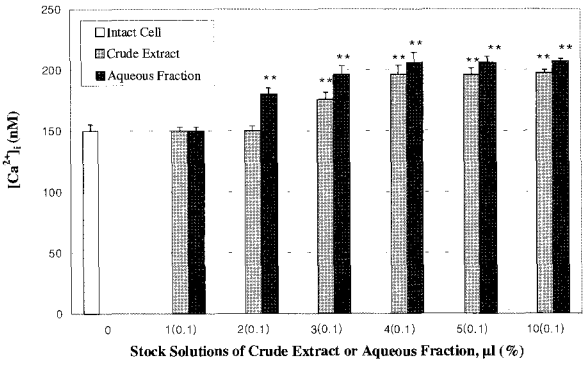

Fig. 7.

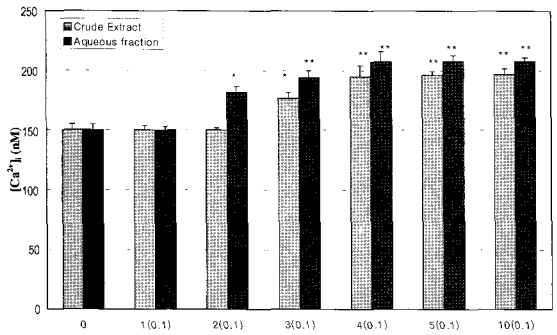

Fig. 8.

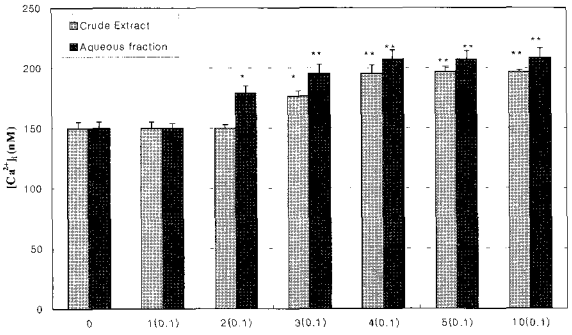

Fig. 9.

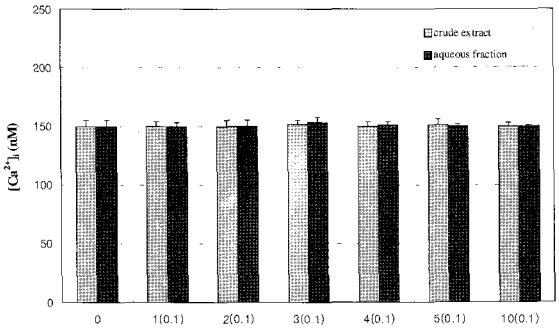

Fig. 10.